



Cite this: *Environ. Sci.: Nano*, 2024, 11, 3721

Received 6th March 2024,  
Accepted 25th July 2024

DOI: 10.1039/d4en00188e

rsc.li/es-nano

Nanoplastics in the environment are a great concern given their nanoscopic size, colloidal stability, and bio-recalcitrant and biomagnifying nature. They are detected ubiquitously in natural and built environments and pose harm to human and ecological health. In this study, we report seminal evidence that suspended nanobubbles can remove nanoplastics when repulsive coulombic forces between nanobubbles and nanoplastics are subdued. Our findings showed that 60% of 100 nm polystyrene latex was eliminated from the water column after stirring in nanobubble solution at the  $pH_{pzc}$  of nanoplastics for 5 min, whereas the controls with no nanobubbles showed no removal. Nanoparticle tracking analysis indicated a 61% decrease in number concentration and 27% increase in particle size in the supernatant due to plastic-bubble attachment. Additionally, the mass concentration of nanoplastics in the float after nanobubble flotation was 123% more than the concentration in the supernatant confirming an upward shuttling of the plastic-bubble aggregate. This study paves the way forward for engineering systems where coagulation and flotation can deliberately contribute to the removal of nanoplastics with the utility of nanobubbles.

## 1. Introduction

Nanoplastics (NPs, *i.e.*, typically defined as polymeric particulates <1000 nm) form in the environment by the weathering of plastic debris due to environmental stressors such as ultraviolet radiation, physical forces, chemical oxidants, and biological degradation.<sup>1–3</sup> They occur after the breakdown of microplastics which are commonly polyethylene, polypropylene, polystyrene (PS), polyvinyl chloride, and polyethylene terephthalate polymers.<sup>4</sup> NPs are ubiquitous in the natural aquatic environment and their

# Emerging investigator series: suspended air nanobubbles in water can shuttle polystyrene nanoplastics to the air–water interface†

Kenneth Mensah,<sup>a</sup> Andre Magdaleno,<sup>b</sup> Sudheera Yaparathne,<sup>a</sup> Sergi Garcia-Segura<sup>b</sup> and Onur G. Apul<sup>b\*</sup>

### Environmental significance

Widespread nanoplastic pollution of the aquatic environment has cascading environmental and public health consequences. The long-term stability of nanoplastics in water further complicates their removal by traditional approaches. The key finding of this study is that suspended nanobubbles in water can shuttle nanoplastics to the air–water interface *via* hetero-aggregation if repulsive coulombic forces are overcome by pH adjustment. Although it is still in its early stages, nanobubble-based water treatment can enable NP removal if technology matures and embraces the intricacies of scaling up. This is the first evidence of nanobubble–nanoplastic floc formation and subsequent flotation, which can lead to utilization of engineered solutions by deploying nanobubbles for nanoplastic remediation when traditional approaches are not able to.

minuscule size and surface charge make them arduous to eliminate.<sup>5–7</sup> NPs exist in seas, rivers, and nature reserves across the globe at 0.3–488  $\mu\text{g L}^{-1}$  levels.<sup>8</sup>

At low trophic levels, NPs can bind to algae or can be directly ingested by aquatic organisms.<sup>9</sup> The nanometric size of nanoplastics enables their permeation of biological membranes unlike larger particles, and then they exert reproductive, developmental, neurological, endocrinal, and intestinal toxicity.<sup>7,10,11</sup> For example, in *Daphnia*, polystyrene NPs stimulate reactive oxygen species generation and decrease antioxidant enzyme activity leading to retardation of the growth rate and reproductive ability, and shorten the lifespan of zooplanktons.<sup>7,12,13</sup> Polystyrene NPs also interfere with the embryonic development of zebrafish, oysters, sea urchins, and mussels causing hormonal disorders, gonadal damage, inflammation, oxidative stress, and an imbalance in energy metabolism.<sup>7,14–18</sup> At higher trophic levels, ingesting NPs is also problematic because they can reduce the viability of HepG2 liver cells and destroy antioxidant capabilities.<sup>19</sup> NPs were detected in human cells and are shown to be cytotoxic to the human reproductive, digestive, and nervous systems by inducing oxidative stress, causing inflammation and metabolic disorders.<sup>4,20,21</sup> In addition, ingestion of NPs may indirectly result in contaminant uptake by leaching of

<sup>a</sup> Department of Civil and Environmental Engineering, University of Maine, Orono, ME 04469, USA. E-mail: onur.apul@maine.edu; Fax: +1 207 581 3888; Tel: +1 207 581 2981

<sup>b</sup> School of Sustainable Engineering and the Built Environment, Arizona State University, Tempe, AZ 85287, USA

† Electronic supplementary information (ESI) available. See DOI: <https://doi.org/10.1039/d4en00188e>



toxic monomers, oligomers, additives, and/or adsorbed micropollutants (*i.e.*, the Trojan horse mechanism).<sup>7,22,23</sup>

These multifaceted implications of NP pollution necessitate urgent and innovative water treatment strategies as they pose ecological and human health risks. Although it is still in its early stages, nanobubble-based water treatment can enable NP removal if technology matures and embraces the intricacies of scaling up. Successful separation of larger plastic debris such as microplastics from water by coarse bubble flotation has been demonstrated in the literature.<sup>24–26</sup> However, the removal of NPs *via* flotation has not been explored yet. Removing ultrafine NPs by coarse bubble flotation is challenging because of the low collision probability between the short-lived coarse bubbles and fine particulates.<sup>27,28</sup> Nanobubbles, on the other hand, are on the same scale as NPs, and they have conspicuously greater retention times in water;<sup>29–31</sup> thus, they present an opportunity for NP flotation.<sup>32,33</sup> Nanobubbles lack buoyancy and remain suspended in solution with Brownian motion as the only mechanism of transport in aqueous solution.<sup>29,34</sup> Suspended nanobubbles can attach to the surface of NPs, improve dissolved air concentration, and result in higher flotation efficiencies. In addition, smaller bubbles adhere more strongly to surfaces than coarser bubbles and hence are less likely to detach from surfaces during flotation.<sup>24,33,35</sup> The enhanced flotation recoveries with nanobubbles may also extend to coarser materials by multiple bubble attachments.<sup>36</sup> For this, we studied the utility of nanobubbles towards NP removal and gained formative mechanistic insights for nanobubble-based flotation.

We report seminal fundamental evidence of nanobubble-based flotation to remove NPs from water by nanobubble–NP hetero-aggregation. The objectives of the study were to: (i) investigate the removal of NPs using nanobubble flotation, (ii) understand the surface chemistry and underlying mechanism of nanobubble–NP attachment, and (iii) study the probability and rate of NP–nanobubble collision, attachment, and flotation. To achieve these objectives, we experimentally tested the influence of pH and stirring speed as independent variables on the plastic–bubble attachment, rising velocity, and removal while providing theoretical computations to explain the results.

## 2. Materials and methods

### 2.1. Nanobubble-based flotation experimental procedure

Information about materials and reagents used in this study is presented in Text S1 in the ESI.† For flotation experiments, 10  $\mu\text{L}$  of 100 nm polystyrene NP latex was added to 40 mL of solution containing or in the absence of nanobubbles reaching a final nanoplastic concentration of 26  $\mu\text{g L}^{-1}$ . The nanobubble solution was produced using a Moleaer XTB 25 nanobubble generator as detailed in Text S1.† The water height of each suspension was 2.4 cm and the diameter of the beaker was 4.6 cm. Each sample was stirred at either 100 rpm ( $Re = 81$ ) or 400 rpm ( $Re = 325$ ) for 5 min using a

Heidolph MR Hei-Tec magnetic stirrer. The stirring rod was cylindrical with 2.5 cm length and 0.7 cm diameter. After stirring, the suspension was observed for the fluid motion in about 5–10 seconds for the meniscus of the suspension to come to rest and be stationary and quiescent. Samples were drawn from the stagnant float and subnatant of the suspension. A plastic syringe was placed at the meniscus of the suspension to collect the float and then at about 2 cm below the meniscus to collect the subnatant. The influence of pH on nanoplastic flotation with nanobubble solution was investigated by adjusting the pH to 3.0, 5.0, and 9.0 using 0.1 M HCl or 0.1 M NaOH. All pH measurements of the solutions are presented in Table S1.† Control experiments were conducted for solutions containing nanobubbles only and NPs only in ultrapure distilled and deionized water (DDI, Barnstead NANOpure Infinity ultrapure water system,  $>18.2 \text{ M}\Omega \text{ cm}$ ). The effect of the velocity gradient on plastic–bubble attachment was examined by adjusting the stirring speed of NPs in nanobubble solution at 100 rpm *vs.* 400 rpm.

### 2.2. Analytical procedures

A Hach DR 6000 UV-vis spectrophotometer was used to measure the nanoplastic concentration at  $\lambda = 249 \text{ nm}$ . The detailed UV-vis spectrophotometry method is described in Text S2 (including the calibration curve in Fig. S1) in the ESI.† The number concentration and size of NPs and nanobubbles were determined by nanoparticle tracking analysis (NTA) using a NanoSight NS300. The solution pH was measured using a MultiLab IDS 4010-3 W, and the zeta potential was quantified using a Zetasizer Nano-ZS. The analytical procedures of these characterization techniques are described in detail in Text S2 of the ESI.† The data points presented are averaged from triplicate experiments with standard error bars. The one-way ANOVA test at 95% confidence interval was used to determine the statistical significance.

## 3. Results and discussion

### 3.1. Nanobubble-based flotation of nanoplastics

Nanobubble and NP solutions looked indistinguishable to the naked eye before and after the flotation experiments. The only visible difference was the appearance of a thin film resembling an immiscible oil layer on water after stirring NPs with nanobubbles at pH 3 (Fig. S2 in the ESI.†). We attributed the formation of this film to the migration of suspended NP–nanobubble flocs to the air–water interface. Fig. 1a presents the mass concentration of NPs measured by UV-vis in the subnatant after 5 min stirring at different pH levels. It should be noted that the detection of NPs by UV-vis was not influenced by the presence of nanobubbles as indicated by the calibration curves presented in Fig. S1 in the ESI.† After stirring the nanobubble solutions with NPs, the concentration of NPs decreased as a function of pH, resulting in removal percentages of 60, 9, 6, and 0% at pH 3.0, 5.0, 6.0, and 9.0, respectively. Conversely, no to little changes were





**Fig. 1** (a) Nanoplastic concentration in the supernatant after stirring at various pH (conditions: initial nanoplastic concentration = 26  $\mu\text{g L}^{-1}$ , stirring speed = 400 rpm, stirring time = 5 min). The  $p$ -values show a statistically significant difference in NP concentration in nanobubble solution vs. DI water. NTA analysis of nano-entities in the supernatant before and after stirring: (b) normalized number concentration at all pH ranges and (c) particle size distributions at pH 3.0.  $C_{T0}$  and  $C_T$  denote the initial and final number concentration, respectively.

noted when the same experiment was conducted in the absence of nanobubbles, yielding NP removal rates of 8, 3, 0, and 0% at pH 3.0, 5.0, 6.0, and 9.0, respectively.

To complement the mass concentration data, NTA analysis was performed, and the changes in the number concentrations were reported. The results from Fig. 1b are affirmative as a consistent decrease in number concentration was observed as the pH decreased to 3.0 while the nanoscopic entity counts at pH 5.0, 6.0, and 9.0 remained relatively unchanged (<20% of the initial concentrations). Specifically, at pH 3.0, a significant decrease of 61% in the

initial NP concentration ( $p$ -value = 0.0025) was observed after stirring the NPs in the nanobubble mixture. This was attributed to the destabilization of nanobubbles and the removal of NPs. However, since NTA does not distinguish nanobubbles from NPs, control experiments with only nanobubbles and only NPs were also conducted at pH 3.0. These control experiments showed 58% and 19% decreases in number concentrations after stirring only nanobubbles and only NPs, respectively. This confirmed that the NPs were relatively stable in DI water during stirring at pH 3.0 but they were destabilized when nanobubbles were in the system. Therefore, the primary mechanism of NP removal was speculated to be hetero-aggregation of nanobubbles with NPs with the subsequent rise of the bubble-particle flocs (*i.e.*, upward sweeping) to the surface of the vessel.

To confirm the discussed results, quantitative analysis of the changes in the number concentration and size distributions of the nanobubbles alone, NPs alone, and NP-nanobubble systems were evaluated. Fig. 1c shows a graph of the NTA number concentration *versus* size, and the area under the curve was integrated by the NTA software to determine the value of the total number concentration written beside each curve. The size distribution of nanobubbles showed polydisperse “peaks and shoulders” ranging from 80 to 300 nm, with a noticeable decline in the intensity of the peaks especially in the 80 to 200 nm range after 5 min of stirring at pH 3.0. The size distribution of NPs, on the other hand, was uniform around 100 nm, and it maintained its monodispersity after stirring despite a slight reduction in the intensity. The curve representing the mixture of NPs and nanobubbles exhibited both the characteristic 100 nm NP peak and the nanobubble “peaks and shoulders”. After stirring at pH 3.0, a notable decrease in the NP peak (at 100 nm intensity) was observed, resulting in a net loss of 106 million entities per mL in the bulk of the NP-nanobubble mixture. Considering the initial number concentration of nanobubble solution, the loss of 65 million entities per mL was assumed to be the removal of nanobubbles yielding a loss of 41 million NPs per mL from water in 5 min. This corresponds to 51% NP removal, and it aligns well with the UV-vis observation, which indicated 60% removal. The NTA micrographs in Fig. S3† further illustrate the changes in the number concentration at pH 3.0. The size measurements with NTA and zeta potential were investigated and discussed in section 3.2 to provide a detailed mechanistic insight into the NP removal in nanobubble solution at pH 3.0.

### 3.2. Mechanistic insights into bubble-plastic attachment and nanoplastic flotation

The changes in size according to NTA analysis after stirring at pH 3.0 are presented in Fig. 2a. It should be noted that the NTA measurements in this section are conducted for the residual nanoscopic entities in bulk suspension (supernatant) after the treatment. The average increase in size by particle aggregation for all other pH values was negligible *i.e.*, <5%



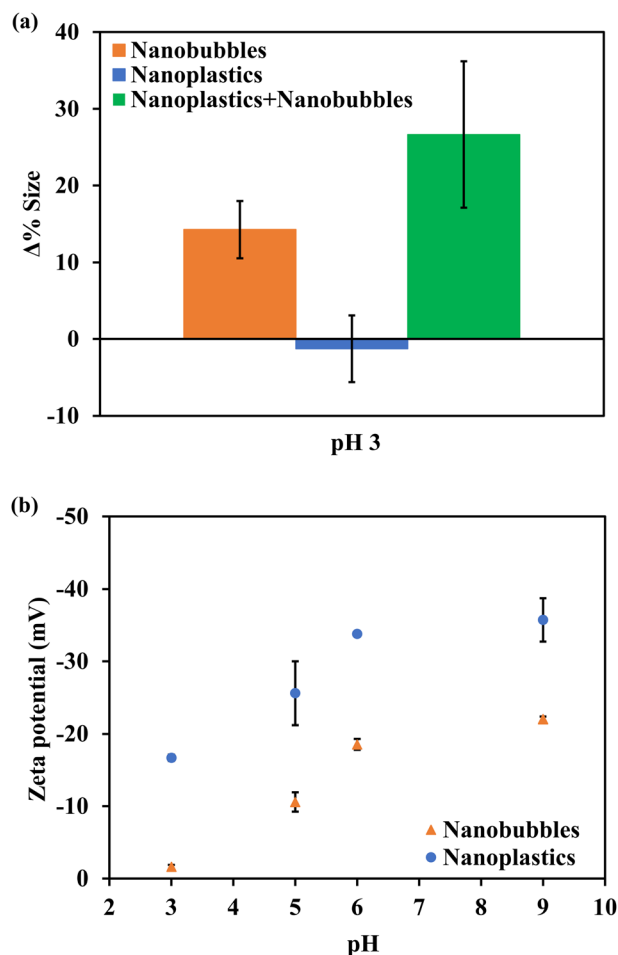


Fig. 2 (a) NTA size analysis of nano-entities in the supernatant after stirring at 400 rpm for 5 min. (b) Zeta potential measurements for nanobubbles and nanoplastics.

(Fig. S4†). Also at pH 3.0, the average size of NPs alone remained relatively unchanged indicating that stirring at pH 3.0 does not cause homo-aggregation of NPs, confirming the findings from NTA and UV-vis spectroscopy. Thus, the 19% loss in NP number concentration when NPs alone were stirred at pH 3 may be attributed to the traveling of NPs that were close to the meniscus of the suspension through the air–water interface to form aerosols due to the vortex created during stirring. On the other hand, the size of nanobubbles without NPs increased by 14%, indicating that the bubbles were destabilized and coalesced. Coalesced bubbles can have sufficient volume to experience buoyancy, causing them to rise to the surface and collapse.<sup>37</sup> This accounts for the 58% loss of nanobubbles when nanobubbles alone were stirred at pH 3. Affirmatively, the NPs in the nanobubble solution showed a 27% increase in size indicating not only the coalescence of bubbles but also floc-forming interactions with NPs. NP–nanobubble flocs can rise to the surface of the bulk water during stirring, resulting in NP flotation. The NP floats can accumulate and be trapped at the air–water interface or

form NP aerosols as the NP–nanobubble flocs burst at the air–water interface.<sup>38</sup> However, no evidence for aerosolization was collected in this study. Additionally, the thin film layer volume was too thin to measure. The increasing size of bubbles and NP–nanobubble flocs were attributed to decreasing repulsive coulombic forces between NPs and nanobubbles at pH 3.0. As shown in Fig. 2b, the zeta potential diminished with decreasing pH, leading to an almost complete charge neutralization for nanobubbles and notable compression of the electric double layer for NPs.<sup>39</sup> At unmodified pH, both NPs and nanobubbles were negatively charged with zeta potentials of  $-33.8$  mV and  $-17.8$  mV, respectively. The NP zeta potential was subdued to  $-16.7$  mV at pH 3.0, while nanobubbles had nearly no charge *i.e.*,  $-1.6$  mV at pH 3.0. Therefore, the subdued electrostatic repulsion at pH 3.0 is ascribed to enabling the attachment of NPs and nanobubbles.<sup>24</sup>

### 3.3. Ratio, density, size, and rising velocity of nanoplastic–nanobubble aggregates

To further establish the mechanistic insights regarding the nanobubble-based NP flotation, the changes in density, concentration, and size as well as nanoplastic–nanobubble attachment and rising velocities were computed using the equations in Text S3.†<sup>39–41</sup> According to the NTA analysis, nanobubbles and NPs have average diameters of 137 and 109 nm, respectively. The densities of polystyrene NPs and air nanobubbles were assumed to be  $1070$  and  $409$  kg m<sup>-3</sup>, respectively.<sup>40–42</sup> It should be noted that the density of nanobubbles is scarcely reported in the literature and future research on nanobubble density can contribute to enhancing the accuracy of computational results. Based on these assumptions, the minimum volume of gas ( $\phi_g$ ) required to float all the NPs was computed as  $6.56 \times 10^{-6}$  mL L<sup>-1</sup>. To determine whether enough gas volume in nanobubbles is present at pH 3.0, the critical diameter required for the nanobubbles, to overcome their Brownian motion and rise, was calculated to be 488 nm. This implies that at least 3.6 nanobubbles are needed to come together to reach the critical rising diameter. In addition, the number of nanobubbles that coalesced and traveled upwards was computed as 18 million per mL. The total volume occupied by 18 million nanobubbles per mL is  $1.11 \times 10^{-3}$  mL L<sup>-1</sup> (assuming that the nanobubbles are perfect spheres), which is three orders of magnitude greater than the minimum gas volume,  $\phi_g$ , required for 100% NP removal. This implies that the small gas volume packed in nanobubbles is not limiting the success of NP flotation. For our case, the generation of at least 112 million nanobubbles per mL could ensure complete NP removal theoretically. Lastly, based on the assumption that 3.6 nanobubbles coalesced at pH 3.0 to form “the rising nanobubbles with critical size”, our results indicate that each “rising nanobubble” attaches to 2.3 NPs (assuming 100% collision-attachment efficiency). Analogously, we suppose that the total volume of residual nanobubbles in the bulk





phase after stirring at pH 3 ( $3.7 \times 10^{15} \text{ nm}^3$ ) is subtracted from the initial total volume of nanobubbles present before stirring ( $6.0 \times 10^{15} \text{ nm}^3$ ). In that case,  $2.3 \times 10^{15} \text{ nm}^3$  of nanobubbles is estimated to have traveled upwards to the air–water interface during stirring, representing 38% loss of the initial nanobubble volume. Assuming the nanobubbles floated to the surface at the critical size (488 nm), 37.2 million bubbles rose to cause NP flotation. This implies that, in this case, 4.4 NPs were attached to a coalesced-rising bubble during flotation.

The coalesced nanobubbles are computed to rise at a velocity of  $2.97 \mu\text{m min}^{-1}$  while NPs settled slowly at  $0.03 \mu\text{m min}^{-1}$ . However, when they attach to form NP–nanobubble flocs, they are computed to rise at a speed of  $2.93 \mu\text{m min}^{-1}$  (if 2.3 NPs attached to the rising nanobubbles) or  $2.90 \mu\text{m min}^{-1}$  (if 4.4 NPs attached to the rising nanobubbles). The rising velocities of NP–nanobubble flocs are two orders of magnitude greater than the settling rate of NPs, indicating that attaching nanobubbles to NPs will significantly accelerate NP mobility. Moreover, in a typical flotation cell, coarse bubbles provide additional rising velocity as they attach to the NP–nanobubble flocs. Nevertheless, the computed rising velocities of the NP–nanobubble flocs are still not enough to achieve flotation in a 2.4 cm suspension height within 5 min. This indicates that incidental vertical fluid mixing enhanced the rising of NP–nanobubble flocs leading to flotation in 5 min due to the vortex created during stirring. Control experiments under static conditions (no stirring for 5 min) confirmed the impact of stirring on NP–nanobubble attachment and flotation (Fig. S5†). There was no difference between the subnatant and float concentrations when there was no mixing, but an increase in NP and NP–nanobubble floc size occurred. This signifies that the agglomeration of the nano-entities proceeds immediately after the electric double layer is overcome without stirring. However, the agglomerated particles could not rise to the surface in 5 min, and hence no increase in the float number concentration occurred due to the lack of the external rising force created by stirring. The rise of NP–nanobubble flocs during stirring was confirmed by analyzing and comparing the concentration and size of NPs in the float and subnatant after stirring (Fig. S6†). In the NP-only control, the mass and number concentrations (Fig. S6a and b†) and size of NPs (Fig. S6c†) in the float were the same as those of the NPs in the suspension after stirring at pH 3.0 and 6.0 for 5 and 30 min. This indicates that without nanobubbles, NPs do not accumulate in the froth. Similarly, when NPs were stirred in nanobubbles at unmodified pH for 5 and 30 min, no significant difference in the float and subnatant concentration (Fig. S6a and b†) and size (Fig. S6c†) was observed in both stirring durations. This indicates that the presence of repulsive coulombic forces deters the hetero-aggregation required for flotation to occur even if the stirring duration is extended. In contrast, in the nanobubble solution at pH 3.0, the mass concentration of NPs in the float after treatment was 123% more than that in the subnatant (Fig.

S6a and b†) after stirring for 5 min. There was likewise a significant 27% increase in size (Fig. S6c†) which was elaborated earlier. This difference between the float and subnatant upholds the inferences that the NPs attach to nanobubbles at pH 3.0 and rise to the air–water interface during stirring.

The NP–nanobubble attachment can occur *via* the formation of a three-phase wetting perimeter and a spontaneous rupture of a fluid film between the bubble and particle. This attachment is propelled by hydrophobic forces and affected by the contact angle between particles and bubbles, liquid surface tension, and particle surface properties like zeta potential and roughness. Alternatively, contactless flotation could take place, which is influenced by attractive interparticle forces overcoming repulsive forces.<sup>24,43,44</sup> The former mechanism of nanobubble–NP attachment is assumed to have taken place here since the thickness of the electric double layer was the driver of NP–nanobubble attachment. The rate at which the NPs and nanobubbles collide and attach is also governed by the induced velocity gradient during mixing.<sup>39</sup> This was studied experimentally by varying the stirring speed at 400 and 100 rpm. To improve the chances of NP–nanobubble collision, attachment, and flotation, 100 and 400 rpm stirring were selected to represent slow (less turbulent) and fast (more turbulent) agitation regimes, respectively. The equations for calculating the velocity gradient, collision frequency, and the rate of attachment are in Text S4† and the results are discussed in Text S5.† The findings indicate the role of hydrodynamic shearing forces from agitation that may require optimization for the envisioned applications and NP characterization. Stirring at 100 rpm showed better hetero-aggregation (bigger floc size in both float and subnatant) and flotation (higher NP removal and float concentration) than 400 rpm. However, the NP removal at 100 rpm *versus* 400 rpm was not statistically different in terms of both mass concentration ( $p$ -value = 0.516) and number concentration ( $p$ -value = 0.941). A lesser floc breakage in the bulk and a lower floc collapse rate at the air–water interface may account for this improvement at 100 rpm. This also demonstrates that NPs and nanobubbles can attach and float under minimal stirring indicating the potential low energy demand of the nanobubble-enabled flotation of nanoplastics.

## 4. Conclusion

The findings from this work show that nanobubbles can attach to NPs once the electric double layer is subdued. Nevertheless, flotation only occurs when the system is agitated by stirring due to incidental vertical fluid mixing. A slow mixing regime at 100 rpm favored both hetero-aggregation of NP–nanobubbles (*i.e.*, bigger floc size) and flotation compared to 400 rpm; however, the efficiencies at 100 and 400 rpm were not statistically significantly different. The floated NPs were speculated to be either trapped at the



air–water interface increasing the float concentration or converted into aerosols as the NP–nanobubble flocs burst at the surface. This suggests that the floated NP concentration may not always balance out the residual NP concentration remaining in the supernatant after flotation. The fundamental underlying principles revealed by this work are crucial to comprehending the mechanisms of NP flotation and a key step to NP removal from real water and wastewater. The technique demonstrated in this work has potential to work as a standalone treatment process for removing nanoplastics from hyperclean effluents. Moreover, NP–nanobubble attachment can serve as an ancillary step to the conventional coarse bubble flotation and reduce the amount of surfactant, frother, and collector used for flotation. However, issues such as low solution pH required, how long the aggregates are held together, and the aging and shapes of NPs must be taken into practical consideration. Thus, further studies are required to determine the interactions between nanobubbles and NPs of different polymers, sizes, shapes, hetero-aggregation, and flotation kinetics. Moreover, coagulants like alum can also be investigated as a potential alternative to the use of acid. Additionally, investigation must be done to determine if the NP removal can be improved by increasing the nanobubble concentration or by introducing flotation reagents such as collectors, frothers, and modifiers. Future studies must also investigate if aerosolization of nanoplastics occurs during flotation and engineer ways to curb this problem. Scaling up the technology will require engineering considerations such as the need for an additional nanobubble flotation tank, the size and shape of the tank required, space to accommodate the physical footprint and the type and speed of suitable propellers, as well as cost–benefit analysis to determine its feasibility.

## Data availability

The data underlying this study are available in the published article and its ESI.†

## Conflicts of interest

There are no conflicts to declare.

## Acknowledgements

The authors are thankful for the financial support provided by the NASA EPSCoR Cooperative agreement number: EP-23-03 and Federal Award No: 80NSSC22M0168. Any opinions, findings, and conclusions or recommendations expressed in this material are those of the authors and do not necessarily reflect the views of the National Aeronautics and Space Administration or of the Maine Space Grant Consortium. The authors thank Micheal Mason's Lab for their support in dynamic light scattering measurements and John Graf and Emily Matula for their critical input during research meetings.

## References

- 1 H. P. H. Arp, D. Kühnel, C. Rummel, M. Macleod, A. Potthoff, S. Reichelt, E. Rojo-Nieto, M. Schmitt-Jansen, J. Sonnenberg, E. Toorman and A. Jahnke, Weathering Plastics as a Planetary Boundary Threat: Exposure, Fate, and Hazards, *Environ. Sci. Technol.*, 2021, 7246–7255, DOI: [10.1021/acs.est.1c01512](https://doi.org/10.1021/acs.est.1c01512).
- 2 L. M. Hernandez, N. Yousefi and N. Tufenkji, Are There Nanoplastics in Your Personal Care Products?, *Environ. Sci. Technol. Lett.*, 2017, 4(7), 280–285, DOI: [10.1021/acs.estlett.7b00187](https://doi.org/10.1021/acs.estlett.7b00187).
- 3 J. Gigault, A. Halle, M. Baudrimont, P. Y. Pascal, F. Gauffre, T. L. Phi, H. El Hadri, B. Grassl and S. Reynaud, Current Opinion: What Is a Nanoplastic?, *Environ. Pollut.*, 2018, 1030–1034, DOI: [10.1016/j.envpol.2018.01.024](https://doi.org/10.1016/j.envpol.2018.01.024).
- 4 S. Yang, M. Li, R. Y. C. Kong, L. Li, R. Li, J. Chen and K. P. Lai, Reproductive Toxicity of Micro- and Nanoplastics, *Environ. Int.*, 2023, 177, 108002, DOI: [10.1016/j.envint.2023.108002](https://doi.org/10.1016/j.envint.2023.108002).
- 5 J. P. da Costa, P. S. M. Santos, A. C. Duarte and T. Rocha-Santos, (Nano)Plastics in the Environment - Sources, Fates and Effects, *Sci. Total Environ.*, 2016, 15–26, DOI: [10.1016/j.scitotenv.2016.05.041](https://doi.org/10.1016/j.scitotenv.2016.05.041).
- 6 J. J. Alava, A. Jahnke, M. Bergmann, G. V. Aguirre-Martínez, L. Bendell, P. Calle, G. A. Domínguez, E. M. Faustman, J. Falman, T. N. Kazmiruk, N. Klasios, M. T. Maldonado, K. McMullen, M. Moreno-Báez, G. Öberg, Y. Ota, D. Price, W. J. Shim, A. Tirapé, J. M. Vandenberg, Z. Zoveidadianpour and J. Weis, A Call to Include Plastics in the Global Environment in the Class of Persistent, Bioaccumulative, and Toxic (PBT) Pollutants, *Environ. Sci. Technol.*, 2023, 8185–8188, DOI: [10.1021/acs.est.3c02476](https://doi.org/10.1021/acs.est.3c02476).
- 7 K. Yin, Y. Wang, H. Zhao, D. Wang, M. Guo, M. Mu, Y. Liu, X. Nie, B. Li, J. Li and M. Xing, A Comparative Review of Microplastics and Nanoplastics: Toxicity Hazards on Digestive, Reproductive and Nervous System, *Sci. Total Environ.*, 2021, 774, 145758, DOI: [10.1016/j.scitotenv.2021.145758](https://doi.org/10.1016/j.scitotenv.2021.145758).
- 8 C. Shi, Z. Liu, B. Yu, Y. Zhang, H. Yang, Y. Han, B. Wang, Z. Liu and H. Zhang, Emergence of Nanoplastics in the Aquatic Environment and Possible Impacts on Aquatic Organisms, *Sci. Total Environ.*, 2024, 906, 167404, DOI: [10.1016/j.scitotenv.2023.167404](https://doi.org/10.1016/j.scitotenv.2023.167404).
- 9 Q. Chen, J. Reisser, S. Cunsolo, C. Kwadijk, M. Kotterman, M. Proietti, B. Slat, F. F. Ferrari, A. Schwarz, A. Levivier, D. Yin, H. Hollert and A. A. Koelmans, Pollutants in Plastics within the North Pacific Subtropical Gyre, *Environ. Sci. Technol.*, 2018, 52(2), 446–456, DOI: [10.1021/ACS.EST.7B04682/ASSET/IMAGES/LARGE/ES-2017-04682T\\_0003.JPEG](https://doi.org/10.1021/ACS.EST.7B04682/ASSET/IMAGES/LARGE/ES-2017-04682T_0003.JPEG).
- 10 M. K. Devi, N. Karmegam, S. Manikandan, R. Subbaiya, H. Song, E. E. Kwon, B. Sarkar, N. Bolan, W. Kim, J. Rinklebe and M. Govarthan, Removal of Nanoplastics in Water Treatment Processes: A Review, *Sci. Total Environ.*, 2022, 845, 157168, DOI: [10.1016/j.scitotenv.2022.157168](https://doi.org/10.1016/j.scitotenv.2022.157168).
- 11 H. Lai, X. Liu and M. Qu, Nanoplastics and Human Health: Hazard Identification and Biointerface, *Nanomaterials*, 2022, 12(8), 1298, DOI: [10.3390/nano12081298](https://doi.org/10.3390/nano12081298).



- 12 C. B. Jeong, H. M. Kang, M. C. Lee, D. H. Kim, J. Han, D. S. Hwang, S. Souissi, S. J. Lee, K. H. Shin, H. G. Park and J. S. Lee, Adverse Effects of Microplastics and Oxidative Stress-Induced MAPK/Nrf2 Pathway-Mediated Defense Mechanisms in the Marine Copepod *Paracyclops* Nana, *Sci. Rep.*, 2017, 7(1), 1–11, DOI: [10.1038/srep41323](#).
- 13 X. Sun, B. Chen, Q. Li, N. Liu, B. Xia, L. Zhu and K. Qu, Toxicities of Polystyrene Nano- and Microplastics toward Marine Bacterium *Halomonas Alkaliphila*, *Sci. Total Environ.*, 2018, **642**, 1378–1385, DOI: [10.1016/j.scitotenv.2018.06.141](#).
- 14 Z. Duan, X. Duan, S. Zhao, X. Wang, J. Wang, Y. Liu, Y. Peng, Z. Gong and L. Wang, Barrier Function of Zebrafish Embryonic Chorions against Microplastics and Nanoplastics and Its Impact on Embryo Development, *J. Hazard. Mater.*, 2020, **395**, 122621, DOI: [10.1016/j.jhazmat.2020.122621](#).
- 15 J. Wang, W. Qiu, H. Cheng, T. Chen, Y. Tang, J. T. Magnuson, X. Xu, E. G. Xu and C. Zheng, Caught in Fish Gut: Uptake and Inflammatory Effects of Nanoplastics through Different Routes in the Aquatic Environment, *ACS ES&T Water*, 2023, 4(1), 91–102, DOI: [10.1021/acsestwater.3c00392](#).
- 16 A. F. Pedersen, D. N. Meyer, A. M. V. Petriv, A. L. Soto, J. N. Shields, C. Akemann, B. B. Baker, W. L. Tsou, Y. Zhang and T. R. Baker, Nanoplastics Impact the Zebrafish (*Danio Rerio*) Transcriptome: Associated Developmental and Neurobehavioral Consequences, *Environ. Pollut.*, 2020, **266**, 115090, DOI: [10.1016/j.envpol.2020.115090](#).
- 17 X. Xie, T. Deng, J. Duan, J. Xie, J. Yuan and M. Chen, Exposure to Polystyrene Microplastics Causes Reproductive Toxicity through Oxidative Stress and Activation of the P38 MAPK Signaling Pathway, *Ecotoxicol. Environ. Saf.*, 2020, **190**, 110133, DOI: [10.1016/j.ecoenv.2019.110133](#).
- 18 C. González-Fernández, K. Tallec, N. Le Goïc, C. Lambert, P. Soudant, A. Huvet, M. Suquet, M. Berchel and I. Paul-Pont, Cellular Responses of Pacific Oyster (*Crassostrea Gigas*) Gametes Exposed in Vitro to Polystyrene Nanoparticles, *Chemosphere*, 2018, **208**, 764–772, DOI: [10.1016/j.chemosphere.2018.06.039](#).
- 19 Y. He, J. Li, J. Chen, X. Miao, G. Li, Q. He, H. Xu, H. Li and Y. Wei, Cytotoxic Effects of Polystyrene Nanoplastics with Different Surface Functionalization on Human HepG2 Cells, *Sci. Total Environ.*, 2020, **723**, 138180, DOI: [10.1016/j.scitotenv.2020.138180](#).
- 20 X. Song, L. Du, L. Sima, D. Zou and X. Qiu, Effects of Micro(Nano)Plastics on the Reproductive System: A Review, *Chemosphere*, 2023, **336**, 139138, DOI: [10.1016/j.chemosphere.2023.139138](#).
- 21 A. Ragusa, A. Svelato, C. Santacroce, P. Catalano, V. Notarstefano, O. Carnevali, F. Papa, M. C. A. Rongioletti, F. Baiocco, S. Draghi, E. D'Amore, D. Rinaldo, M. Matta and E. Giorgini, Plasticenta: First Evidence of Microplastics in Human Placenta, *Environ. Int.*, 2021, **146**, 106274, DOI: [10.1016/j.envint.2020.106274](#).
- 22 O. S. Alimi, J. Farner Budarz, L. M. Hernandez and N. Tufenkji, Microplastics and Nanoplastics in Aquatic Environments: Aggregation, Deposition, and Enhanced Contaminant Transport, *Environ. Sci. Technol.*, 2018, 1704–1724, DOI: [10.1021/acs.est.7b05559](#).
- 23 P. R. Rout, A. Mohanty, P. Aastha, A. Sharma, M. Miglani, D. Liu and S. Varjani, Micro- and Nanoplastics Removal Mechanisms in Wastewater Treatment Plants: A Review, *J. Hazard. Mater. Adv.*, 2022, **6**, 100070, DOI: [10.1016/j.hazadv.2022.100070](#).
- 24 B. Swart, A. Pihlajamäki, Y. M. John Chew and J. Wenk, Microbubble-Microplastic Interactions in Batch Air Flotation, *Chem. Eng. J.*, 2022, **449**, 137866, DOI: [10.1016/j.cej.2022.137866](#).
- 25 O. Kökkiliç, S. Mohammadi-Jam, P. Chu, C. Marion, Y. Yang and K. E. Waters, Separation of Plastic Wastes Using Froth Flotation – An Overview, *Adv. Colloid Interface Sci.*, 2022, **308**, 102769, DOI: [10.1016/j.cis.2022.102769](#).
- 26 C. Q. Wang, H. Wang, J. G. Fu and Y. N. Liu, Flotation Separation of Waste Plastics for Recycling-A Review, *Waste Manage.*, 2015, **41**, 28–38, DOI: [10.1016/j.wasman.2015.03.027](#).
- 27 D. Tao, Recent Advances in Fundamentals and Applications of Nanobubble Enhanced Froth Flotation: A Review, *Miner. Eng.*, 2022, 107554, DOI: [10.1016/j.mineng.2022.107554](#).
- 28 C. Li and H. Zhang, A Review of Bulk Nanobubbles and Their Roles in Flotation of Fine Particles, *Powder Technol.*, 2022, 618–633, DOI: [10.1016/j.powtec.2021.10.004](#).
- 29 A. J. Atkinson, O. G. Apul, O. Schneider, S. Garcia-Segura and P. Westerhoff, Nanobubble Technologies Offer Opportunities to Improve Water Treatment, *Acc. Chem. Res.*, 2019, 52(5), 1196–1205, DOI: [10.1021/acs.accounts.8b00606](#).
- 30 Y. Kyuichi, Mechanism for Stability of Ultrafine Bubbles, *Japanese Journal of Multiphase Flow*, 2016, **30**(1), 19–26, DOI: [10.3811/jjmf.30.19](#).
- 31 S. Yaparathne, Z. E. Doherty, A. L. Magdaleno, E. E. Matula, J. D. MacRae, S. Garcia-Segura and O. G. Apul, Effect of Air Nanobubbles on Oxygen Transfer, Oxygen Uptake, and Diversity of Aerobic Microbial Consortium in Activated Sludge Reactors, *Bioresour. Technol.*, 2022, **351**, 127090, DOI: [10.1016/j.biortech.2022.127090](#).
- 32 F. Zhang, L. Sun, H. Yang, X. Gui, H. Schönherr, M. Kappl, Y. Cao and Y. Xing, Recent Advances for Understanding the Role of Nanobubbles in Particles Flotation, *Adv. Colloid Interface Sci.*, 2021, **291**, 102403, DOI: [10.1016/j.cis.2021.102403](#).
- 33 C. Li and H. Zhang, Surface Nanobubbles and Their Roles in Flotation of Fine Particles – A Review, *J. Ind. Eng. Chem.*, 2022, 37–51, DOI: [10.1016/j.jiec.2021.11.009](#).
- 34 E. P. Favvas, G. Z. Kyzas, E. K. Efthimiadou and A. C. Mitropoulos, Bulk Nanobubbles, Generation Methods and Potential Applications, *Curr. Opin. Colloid Interface Sci.*, 2021, **54**, 101455, DOI: [10.1016/j.cocis.2021.101455](#).
- 35 J. Ralston, D. Fornasiero and R. Hayes, Bubble-Particle Attachment and Detachment in Flotation, *Int. J. Miner. Process.*, 1999, **56**, 133–164, DOI: [10.1016/S0301-7516\(98\)00046-5](#).
- 36 S. Calgaroto, A. Azevedo and J. Rubio, Flotation of Quartz Particles Assisted by Nanobubbles, *Int. J. Miner. Process.*, 2015, 137, 64–70, DOI: [10.1016/j.minpro.2015.02.010](#).
- 37 M. Soyluoglu, D. Kim, Y. Zaker and T. Karanfil, Stability of Oxygen Nanobubbles under Freshwater Conditions, *Water Res.*, 2021, **206**, 117749, DOI: [10.1016/j.watres.2021.117749](#).
- 38 H. Lhuissier and E. Villermaux, Bursting Bubble Aerosols, *J. Fluid Mech.*, 2012, **696**, 5–44, DOI: [10.1017/jfm.2011.418](#).



- 39 J. C. Crittenden, R. R. Trussell, D. W. Hand, K. J. Howe and G. Tchobanoglous, *MWH's Water Treatment: Principles and Design*, John Wiley & Sons, 3rd edn, 2012.
- 40 B. Kuizenga, T. Van Emmerik, K. Waldschläger and M. Kooi, Will It Float? Rising and Settling Velocities of Common Macroplastic Foils, *ACS ES&T Water*, 2022, 2(6), 975–981, DOI: [10.1021/acsestwater.1c00467](https://doi.org/10.1021/acsestwater.1c00467).
- 41 K. Waldschläger, M. Born, W. Cowger, A. Gray and H. Schüttrumpf, Settling and Rising Velocities of Environmentally Weathered Micro- and Macroplastic Particles, *Environ. Res.*, 2020, **191**, 110192, DOI: [10.1016/j.envres.2020.110192](https://doi.org/10.1016/j.envres.2020.110192).
- 42 Z. Che and P. E. Theodorakis, Formation, Dissolution and Properties of Surface Nanobubbles, *J. Colloid Interface Sci.*, 2017, **487**, 123–129, DOI: [10.1016/j.jcis.2016.10.027](https://doi.org/10.1016/j.jcis.2016.10.027).
- 43 B. V. Derjaguin, S. S. Dukhin and N. N. Rulyov, Kinetic Theory of Flotation of Small Particles, *Surf. Colloid Sci.*, 1984, **13**, 71–113, DOI: [10.1007/978-1-4615-7972-4\\_2/COVER](https://doi.org/10.1007/978-1-4615-7972-4_2/COVER).
- 44 Y. Xing, X. Gui, L. Pan, B. Pinchasik, Y. Cao, J. Liu, M. Kappl and H. J. Butt, Recent Experimental Advances for Understanding Bubble-Particle Attachment in Flotation, *Adv. Colloid Interface Sci.*, 2017, **246**, 105–132, DOI: [10.1016/J.CIS.2017.05.019](https://doi.org/10.1016/J.CIS.2017.05.019).

